ELSEVIER

Journal of Molecular Structure (Theochem) 664-665 (2003) 189–196

THEO CHEM

www.elsevier.com/locate/theochem

Theoretical study of the kinetics of the hydrogen abstraction reaction $H_2O_2 + O(^3P) \rightarrow OH + HO_2$

Y. Tarchouna[a], M. Bahri[a,*], N. Jaïdane[a], Z. Ben Lakhdar[a], J.P. Flament[b]

[a]*Laboratoire de Spectroscopie Atomique Moléculaire et Applications, Département de Physique, Faculté des Sciences, Université Tunis-El Manar, le Belvédère 1060, Tunis, Tunisia*

[b]*Laboratoire de Physique des Atomes, Lasers et Molécules, CERLA, Université des Sciences et Technologies de Lille 1, 59655 villeneuve-d'Ascq, cedex, France*

Received 11 July 2003; accepted 1 September 2003

Abstract

Ab initio calculation was carried out to determine the electronic structure of reactants, products and transition state involved in the title reaction. The classical barrier height was predicted to be 8.2 kcal/mol. The ab initio results were used with the transition state theory to evaluate the rate constant for the studied reaction over the range of temperature $300 \leq T \leq 2000$ K. Tunneling corrections are considered through the evaluation of the transmission coefficient by the Wigner and the Zero Curvature Tunneling methods. Calculated rate constants are compared to available experimental ones. A reasonable agreement between calculated and measured rate constants was found.

Keywords: Atmospheric chemistry; Ab initio; Transition state; Kinetics

1. Introduction

The hydroxyl radical OH is one of the most important chemical entities in the atmospheric chemistry because of its high reactivity with many compounds. It is known to act in the troposphere as a detergent. The self-cleaning capacity of the troposphere is so affected by the change of OH concentration which depend on the OH loss and production reactions. OH loss and production reactions are practically the most studied ones due to their importance in both combustion and atmospheric chemistry. The OH loss reactions have been more studied than the OH production ones. In this work we are interested in a theoretical study of the kinetics of the production of OH radical via the elementary reaction between the hydrogen peroxide H_2O_2 molecule and the oxygen $O(^3P)$ atom:

$$H_2O_2 + O(^3P) \rightarrow OH + HO_2 \quad (1)$$

There have been numerous experimental measurements of the rate constant of reaction (1) for temperatures below 800 K [1,2]. However, No high temperature experimental data of the rate constants are available for this reaction. We look, in this work, for a high temperature ($T \geq 800$ K)

* Corresponding author. Present address: Département de physique, Faculté des Sciences, B.P. 802, 3018 Sfax, Tunisia.
E-mail address: mohamed.bahri@fss.rnu.tn (M. Bahri).

0166-1280/$ - see front matter © 2003 Elsevier B.V. All rights reserved.
doi:10.1016/j.theochem.2003.09.005

rate constant theoretical data for reaction (1) which can be useful in both combustion and atmospheric chemistry. To reach our goal we performed ab initio transition state calculations of the rate constant $k(T)$ for reaction (1) over the range of temperature $300 \leq T \leq 2000$ K.

In the first part of this work we performed ab initio molecular orbital calculation of the structure, energy and vibrational frequencies of reactants, products and activated complex involved in reaction (1). In the second part we used these ab initio electronic structure results with the Transition State Theory (TST) to evaluate the rate constant k_{TST}(T). We corrected the TST values of $k(T)$ to account for tunneling contribution to the reaction. We compared our results of $k(T)$ to the experimental ones of Stang and Hampson [1] fitted by the expression (in cm^3 $molecule^{-1}$ s^{-1}) $k(T) = 1.58 \times 10^{-17} \times T^2 \times \exp(-2000.8\ K/T)$ for $300 \leq T \leq 800$ K. The comparison between calculated and measured rate constants allowed us to show the importance of tunneling effect in the present reaction and to test the reliability of our high temperature ($T > 800$ K) rate constant results.

2. Computational method

2.1. Electronic structure calculation

All ab initio calculations were performed with the GAMESS program [3] using the cc-pVTZ basis set [4]. Reaction (1) is assumed to take place by the hydrogen abstraction path where a hydrogen atom moves from the H_2O_2 molecule to the oxygen atom leading to HO_2 and OH radicals as it is shown in Fig.1. No symmetry restriction is imposed for all species implied in reaction (1). Each species is taken in its ground state. Minimum energy structure, harmonic vibrational frequencies and Zero Point Energy (ZPE) corrections for reactants, products and transition state H_2O_3 complex are determined at the CASSCF [5] level of calculation. For the closed-shell H_2O_2 system the active space contains six electrons in six orbitals: the three bonding orbitals (σ_{O-O} and two σ_{O-H}) and the three corresponding anti-bonding σ^* orbitals. For the open shell molecular systems the active space contains in addition to all the bonding and the anti-bonding σ^* orbitals the orbital of the unpaired electron of oxygen atom in OH and HO_2 and the orbitals of the two unpaired electrons of O5 atom in H_2O_3. For O(^{3}P) oxygen atom the active space contains four electrons in the three p orbitals (p_x, p_y, p_z). Using the CASSCF wave function at the optimum geometry of each species, the energy was corrected for the remaining electron correlation by the MCQDPT2 method of Nakano [6,7]. All inactive electrons (not correlated in the CASSCF calculation) are included in the MP2 calculation. The Basis Set Superposition Error (BSSE) is estimated using the Boys-Bernardi counterpoise procedure [8]:

$$\begin{aligned}\Delta BSSE &= [E^{O}(O) + E^{H_2O_2}_{H_2O_3}(H_2O_2)] - [E^{H_2O_3}(O) \\ &\quad + E^{H_2O_3}_{H_2O_3}(H_2O_2)] \\ \Delta BSSE &= [E^{H_2O_2}_{H_2O_3}(H_2O_2) - E^{H_2O_3}_{H_2O_3}(H_2O_2)] \\ &\quad + [E^{O}(O) - E^{H_2O_3}(O)] \\ \Delta BSSE &= \Delta BSSE(H_2O_2) + \Delta BSSE(O) \qquad (2)\end{aligned}$$

where the upper index on the MCQDPT2//CASSCF energy E refers to the basis set and the lower one refers to the geometry. $\Delta BSSE(H_2O_2)$ and $\Delta BSSE(O)$ are, respectively, the contribution of each fragment to the total BSSE correction.

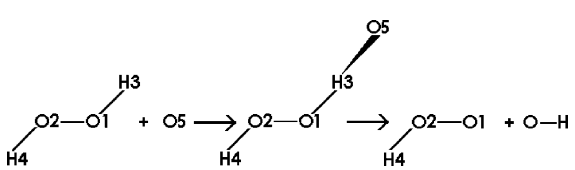

Fig. 1. Assumed mechanism for $H_2O_2 + O$ hydrogen abstraction reaction.

2.2. Rate constant calculation

Rate constants are calculated, as a function of temperature T, in the zero order semi-classical interpolated TST [9]. In this model, the information needed is only available at the reactant (R), the saddle point ($\neq$) and the product (P) and the rate constant is given by:

$$k(T) = \kappa(T) \times k_{TST}(T), \qquad (3)$$

where

$$k_{TST}(T) = \frac{\sigma}{\beta h} \times \frac{Q^{\neq}(T)}{Q^{R}(T)} \times e^{-\beta V^{\neq}} \quad (4)$$

is the conventional TST rate constant without tunneling correction. $\sigma = 2$ (for this reaction) is the symmetry factor accounting for the two possibilities of hydrogen abstraction reaction from H_2O_2·$\beta = 1/K_BT$, K_B is Boltzmann's constant, h is Plank's constant, $Q^R(T)$ and $Q^{\neq}(T)$ are, respectively, the reactant and the transition state partition functions per unit of volume and $V^{\neq}$ is the classical barrier height. To evaluate $Q^R(T)$, $Q^{\neq}(T)$ and $V^{\neq}$ we need the geometry, the energy and the vibrational frequencies of reactants and the activated complex. These quantities are provided by the ab initio part of calculation.

$\kappa(T)$ is a ground state transmission coefficient, which primarily accounts for tunneling correction. In this work we have evaluated this coefficient with two different methods; the Wigner [10] (W) and the ZCT [11] methods. The Wigner transmission coefficient is given by the formula:

$$\kappa(T) = 1 + \frac{1}{24} \times \left| \frac{\hbar \omega^{\neq}}{K_B T} \right|^2 \quad (5)$$

$\omega^{\neq}$ is the imaginary frequency of the transition state.

For details about the ZCT transmission coefficient see the indicated reference.

The two tunneling corrected rate constants are noted, respectively, by $k_{TST/W}$ and $k_{TST/ZCT}$. All the rate constant calculations were done with the POLYRATE7.3.1 program [12].

3. Results and discussion

3.1. Electronic structure calculation

In this section we present our results of the ab initio part of calculation relative to the minimum energy structure, the harmonic vibrational frequencies and the energy of each species implied in reaction (1). As rotational and vibrational partition functions of reactants and the activated complex, which serve to evaluate the TST rate constant, depend, respectively, on the optimized structures and on the vibrational frequencies we test the reliability of our ab initio calculation by comparing our results with the experimental ones.

3.1.1. Minimum energy structure

The calculated CASSCF geometrical parameters for the minimum energy structure of OH, HO_2, H_2O_2 and the activated complex H_2O_3 are given and compared to available experimental ones in Table 1. Inspection of this table shows that CASSCF optimized geometrical parameters of OH and HO_2 radicals and H_2O_2 molecule agree well with the experimental ones. The error ranges from 0.2 to 3% for bond lengths and does not exceed 4.5% for angles. This agreement between calculated and experimental structures indicates that resulting moments of inertia of H_2O_2 molecule, which are useful in calculating rotational partition function, are predicted with a reasonable accuracy.

The bond length R(O2–H4) and the bend angle θ(OOH) at the transition state do not exhibit

Table 1
Calculated CASSCF geometrical parameters of OH, HO_2, H_2O_2 and H_2O_3. (Bond lengths in Å, angles in deg)

System	Parameters[a,b]	CASSCF	Exp[c]
OH	R(O–H)	0.974	0.969
	R(O–O)	1.374	1.335
HO_2	R(O–H)	0.968	0.977
	θ(OOH)	102.69	104.1
H_2O_2	R(O–O)	1.476	1.464
	R(O–H)	0.967	0.965
	θ(O–O–H)	99.11	99.4
	α(HO–O–H)	116.72	111.8
H_2O_3	R(O–O)	1.434	
	R(O1–H3)	1.197	
	R(O2–H4)	0.969	
	R(H3–O5)	1.189	
	θ(O2O1H3)	102.78	
	θ(O1H3O5)	173.17	
	θ(O1O2H4)	101.03	
	α(H4O2O1H3)	93.25	
	α(O5H3O1O2)	−43.43	

[a] See Fig. 1.
[b] R, stretch; θ, bending angle; and α, tortional angle.
[c] Ref. [13].

a significant change with respect to their homologues in H_2O_2 (the relative change is less than 1% for R(O2–H4) and 4% for θ(OOH)). On the other hand the R(O–O) bond length takes an intermediate value between its homologues in H_2O_2 and HO_2 and the dihedral angle α(H4O2O1H3) experiences an important relative change of about 20%. These observations indicate that, although O2 and H4 atoms are not implied directly in the reaction, their geometrical dispositions with respect to reactive atoms O1, H3 and O5 are important in the reactive processes. when comparing the value of R(O1–H3) bond length in H_2O_2 and in H_2O_3 it can be deduced that in order for reaction (1) to take place via the hydrogen abstraction path, the R(O1–H3) bond length must be stretched by about 24%. The bending angle θ(O5H3O1) is predicted to have a value of 173.17°. This indicates that the preferred bringing together of O(^{3}P) atom and H_2O_2 molecule for the reaction is the one where O1, H3 and O5 atoms are almost linear. This has already been observed in other H abstraction reactions [14–18]. Fig. 2 shows the CASSCF isodensity curves of the σ_{O1-H3} orbital in the H_2O_3 activated complex. We note that the probability to find the electrons occupying the σ_{O1-H3} between H3 and O5 atoms is important. So the O1–H3 and H3–O5 bonds at the TS appear ready to be, respectively, broken and formed. This is consistent with the hydrogen abstraction reaction hypothesis and indicates that we located the adequate transition state structure.

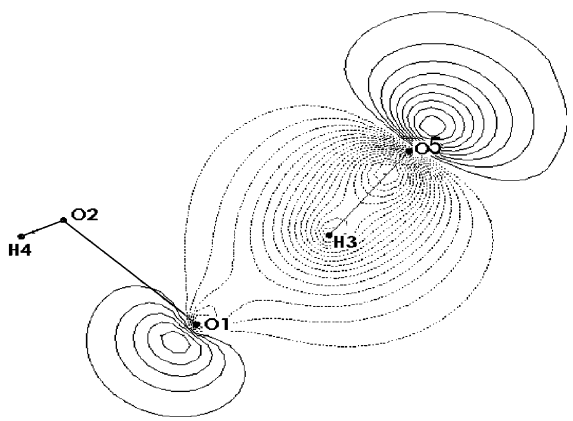

Fig. 2. CASSCF isodensity curves corresponding to the σ(O1–H3) orbital in H_2O_3.

Table 2
Harmonic vibrational frequencies (cm^{-1}) of the equilibrium structure for OH, HO_2, H_2O_2 and H_2O_3

System	CASSCF	Exp[a]
OH	3662.2 (2.5%)[b]	3570
HO_2	915.5 (16.5%)	1097.6
	1482.6 (6.5%)	1391.8
	3719.7 (8.2%)	3436.2
H_2O_2	447.4 (13.9%)	520
	831.4 (6.5%)	890
	1351.0 (6.7%)	1266
	1463.3 (13.0%)	1295
	3740.5 (2.8%)	3610
	3746.0 (2.8%)	3610
H_2O_3	146.5	
	245.6	
	551.2	
	732.4	
	860.1	
	1118.3	
	1441.1	
	3722.7	
	3951.9i	

[a] Ref. [19] for OH, Ref. [20] for HO_2 and Ref. [21] for H_2O_2.
[b] Value in parentheses represents the error (in %) of calculation with respect to experiment.

3.1.2. Vibrational frequencies

The calculated CASSCF harmonic vibrational frequencies of OH, HO_2, H_2O_2 and H_2O_3 are listed with the available experimental ones in Table 2. We note that the disagreement between calculated and experimental frequencies of OH, HO_2 and H_2O_2 ranges from 2.5 to 8% for stretching modes and from 6.5 to 16.5% for other modes. The calculated Hessian matrix of the transition state structure was found to possess only one imaginary frequency $\omega^{\neq}$. The imaginary normal mode is decomposed into the nine internal coordinates by J. A. Boatz and M. S. Gordon's method [22]. The contribution coefficient of each internal coordinate to this mode is given in Table 3. It appears clear that the transition state eigenvector associated to this unique imaginary frequency is primarily a motion of the H3 hydrogen atom between O1 and O5 atoms. This result confirms that we have located the adequate transition state structure in accordance with the hydrogen abstraction reaction hypothesis. Since the imaginary frequency

Table 3
Decomposition of the imaginary normal mode into the nine internal coordinates

Internal coordinate	Contribution coefficient
R(O1–O2)	0.028
R(O1–H3)	−1.010
R(O2–H4)	−0.008
R(H3–O5)	1.004
θ (O2O1H3)	0.008
θ (O1O2H4)	−0.003
θ (O1H3O5)	0.029
α (H4O2O1H3)	0.018
α (O5H3O1O2)	−0.168

governs the width of the classical potential energy barrier along the minimum energy path, it plays an important role in the tunneling calculations. Its magnitude is predicted to be $|\omega^{\neq}| = 3951.9\ \mathrm{cm}^{-1}$ which is large compared to the corresponding value that was previously determined for $H_2O_2 + H$ reaction (2909.9 cm^{-1}) [14] where tunneling was found to be important at ambient temperatures. So for reaction (1) tunneling is expected to be important at ambient temperatures.

3.1.3. Energetics

The calculated MCQDPT2//CASSCF total energies of all species involved in reaction (1) are listed in Table 4. Because the reaction barrier height, which is a very important quantity useful in the rate constant part of calculation, is evaluated from reactants and activated complex total energy values, we need to test the reliability of our energy calculation. The comparison between calculated and experimental values of the reaction energy E_r and

Table 4
Total energies (a.u) of O, OH, HO_2, H_2O_2 and H_2O_3

	CASSCF	MCQDPT2//CASSCF
O(^{3}P)	−74.8057368452	−74.9801086791
OH	−75.4382135126 (5.2)[a]	−75.6419227426
HO_2	−150.2966705032 (8.7)	−150.7143008343
H_2O_2	−150.9393200877 (16.6)	−151.3619406568
H_2O_3	−225.6898254782 (12.6)	−226.3273627781

[a] Values between parentheses are the ZPE corrections in kcal/mol.

Table 5
Calculated reaction energy E_r and bond dissociation energies of the broken (H–OOH) and the formed (H–O) bonds in kcal/mol for reaction (1) (the energy of hydrogen atom calculated at the ROHF level is −0.4998099 a.u.)

	CASSCF	MCQDPT2//CASSCF	Exp.
E_r	6.4 (3.8)[a]	−8.9 (−11.5)	−14.7[b]
E_D(H–OOH)	−89.6 (−81.7)	−92.8 (−84.9)	−87.2[c]
E_D(O–H)	−83.2 (−77.9)	−101.7 (−96.4)	−101.76 ± 0.07[d]

[a] Values between parentheses are the ZPE corrected ones.
[b] Ref. [1].
[c] Ref. [13].
[d] Ref. [23].

the bond dissociation energies E_D(H–OOH) of the broken H–OOH bond and E_D(O–H) of the formed O–H one can be the best test. The calculated values of E_r, E_D(H–OOH) and E_D(O–H) are listed and compared to experimental results in Table 5. The MCQDPT2//CASSCF value of E_r, including ZPE corrections, is −11.5 kcal/mol which is about 3 kcal/mol far from the experimental one. The closest agreement between calculated and experimental values of E_D(H–OOH) and E_D(O–H) was found for the MCQDPT2//CASSCF calculation including ZPE corrections. The disagreement never exceeded 5%.

To take into account various errors and so to improve the accuracy in calculating the barrier height $V^{\neq}$, we evaluated the BSSE correction to $V^{\neq}$. Total energies used to evaluate this correction are given in Table 6. The calculated values of the barrier height without and with consideration of ZPE and BSSE corrections, noted, respectively $V^{\neq}$, $V^{\neq}_{ZPE}$ and

Table 6
CASSCF and MCQDPT2//CASSCF energies (a.u.) used to evaluate the BSSE correction to H_2O_3 total energy

	CASSCF	MCDDPT2/CASSCF
E^{O}(O)	−74.8057368	−74.9801087
$E^{H_2O_3}$(O)	−74.8062456	−74.9835802
$E^{H_2O_2}_{H2O_3}$(H_2O_2)	−150.909991	−151.3321605
$E^{H_2O_3}_{H_2O_3}$(H_2O_2)	−150.9102979	−151.3334254
ΔBSSE(O)	0.3	2.2
ΔBSSE(H_2O_2)	0.2	0.8
ΔBSSE (kcal/mol)	0.5	3.0

Table 7
Calculated barrier height (kcal/mol) for $H_2O_2 + O(^3P)$ reaction

	CASSCF	MCQDPT2//CASSCF
$V^{\neq}$	34.6	9.2
$V^{\neq}_{ZPE}$	30.6	5.2
$V^{\neq}_{ZPE+BSSE}$	31.1	8.2

$V^{\neq}_{ZPE+BSSE}$, are listed in Table 7. The CASSCF calculation predicts for $V^{\neq}$ a value of about 34 kcal/mol which is very high. This was previously observed in a study relative to the $H_2O_2 + H$ hydrogen abstraction reaction. Including electron correlation for the remaining electrons (not included in the CASSCF calculation) via the MCQDPT2 method reduces $V^{\neq}$ by a factor of about 3.7. This confirms the importance of electron correlation in predicting correct barrier heights for reactions. The MCQDPT2//CASSCF value of $V^{\neq}$ is lowered by 4.0 kcal/mol and increased by 3.0 kcal/mol when, respectively, ZPE and BSSE corrections are included. The ZPE and BSSE corrected barrier height $V^{\neq}_{ZPE+BSSE}$ is predicted to have a value of 8.2 kcal/mol. We retain this value to use in the kinetic part of calculation.

3.2. Rate constant calculation

The calculated rate constants for the temperature range from 300 to 2000 K are listed and compared to experimental values in Table 8. Fig. 3 shows the logarithm plot of the modeled rate constants k_{TST}, $k_{TST/W}$, $k_{TST/ZCT}$ and the measured one versus 1000/T(K). First it is notable that the conventional TST rate constants without tunneling, k_{TST}, underestimate the experimental values at low and ambient temperatures. The factor that would be required to bring k_{TST} and the experimental result into agreement ranges from 1929 ($T = 300$ K) to 5 ($T = 800$ K). This indicates that tunnel effect contribution to reaction (1) is assumed to be important even for ambient temperatures. Including Wigner correction to k_{TST} increases the rate constants by a factor less than the required one, and so the $k_{TST/W}$ curve is located between the k_{TST} and the experimental one showing that the Wigner method accounts for only a part of tunneling contribution to

Table 8
Calculated rate constants (cm^3 $molecule^{-1}$ s^{-1}) compared to experimental values

T (K)	k_{TST}	$k_{TST/W}$	$k_{TST/ZCT}$	Exp[a]	Disagreement factor
300	9.38 (−18)[b]	1.50 (−16)	1.57 (−14)	1.81 (−15)	8.7
350	7.61 (−17)	9.12 (−16)	2.40 (−14)	6.40 (−15)	3.8
400	3.78 (−16)	3.56 (−15)	3.64 (−14)	1.71 (−14)	2.1
450	1.35 (−15)	1.04 (−14)	5.46 (−14)	3.76 (−14)	1.4
500	3.85 (−15)	2.46 (−14)	8.08 (−14)	7.25 (−14)	1.1
550	9.23 (−15)	5.03 (−14)	1.18 (−13)	1.26 (−13)	1.1
600	1.95 (−14)	9.24 (−14)	1.68 (−13)	2.03 (−13)	1.2
650	3.72 (−14)	1.56 (−13)	2.35 (−13)	3.08 (−13)	1.3
700	6.56 (−14)	2.46 (−13)	3.24 (−13)	4.46 (−13)	1.4
750	1.08 (−13)	3.68 (−13)	4.37 (−13)	6.19 (−13)	1.4
800	1.70 (−13)	5.28 (−13)	5.81 (−13)	8.32 (−13)	1.4
850	2.55 (−13)	7.30 (−13)	7.58 (−13)		
900	3.68 (−13)	9.81 (−13)	9.75 (−13)		
950	5.16 (−13)	1.29 (−12)	1.24 (−12)		
1000	7.03 (−13)	1.65 (−12)	1.55 (−12)		
1100	9.34 (−13)	2.08 (−12)	1.91 (−12)		
1200	1.22 (−12)	2.57 (−12)	2.34 (−12)		
1300	1.96 (−12)	3.79 (−12)	3.39 (−12)		
1500	2.97 (−12)	5.33 (−12)	4.74 (−12)		
2000	4.29 (−12)	7.24 (−12)	6.42 (−12)		

[a] Ref. [1].
[b] Powers of 10 are between parentheses.

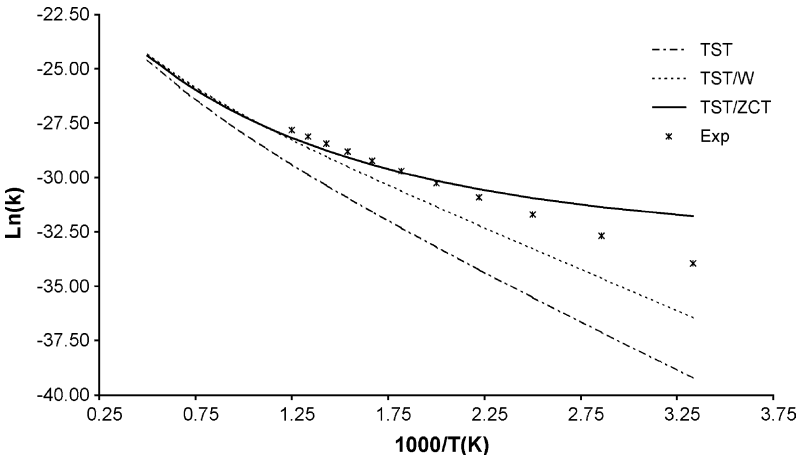

Fig. 3. Plot of logarithm of the calculated and the measured rate constants (cm^3 $molecule^{-1}$ s^{-1}) vs 1000/T(K).

reaction (1). This is due to the fact that Wigner's method only takes into account the effect of the width (not the height) of the minimum energy path, via the value of $\omega^{\neq}$ (see equation 5), in evaluating the tunnel contribution. For $300 \leq T \leq 500$ our rate constants calculation based on the ZCT method overestimates the experimental ones by a factor ranging from 8.7 to 1.1. As the experimental uncertainty factor is about 3.0 [24], the good agreement between modeled and experimental rate constants is found for ZCT method for $500 < T \leq 800$ for where the calculated rate constants underestimate the experimental ones by a factor remaining near the unity (ranging from 1.1 to 1.4). This agreement, specially for $T \geq 500$ K supports the reliability of our rate constant results for high temperatures ($T > 800$ K) for which there are no experimental measurements.

4. Conclusion

We have used the ab initio molecular orbital CASSCF method, to determine the electronic structure of reactants, products and saddle point involved in $H_2O_2 + O(^3P)$ reaction. The magnitude of the unique imaginary frequency of the H_2O_3 activated complex is predicted to have a value of $3951.9\ cm^{-1}$. Using the correlated MCQDPT2//CASSCF method and including ZPE and BSSE corrections the predicted value of the barrier height is 8.2 kcal/mol. The ab initio electronic structure results are used, after being tested, with the TST to evaluate the rate constants of the studied reaction for temperatures ranging from 300 to 2000 K. A large disagreement between calculated rate constants k_{TST} without tunneling contribution and the experimental ones was found for low and ambient temperatures. Tunnel effect for reaction (1) is predicted to be important even for ambient temperatures. We have evaluated tunneling corrections to k_{TST} using the Wigner and the zero curvature tunneling methods. Wigner's method was found to be not sufficient to bring modeled and experimental rate constants into agreement because it accounts for only a small part of tunneling contribution to reaction (1). However, the ZCT method predicts rate constants with a factor of the same order of magnitude as the experimental uncertainty one for almost all considered temperatures. A good agreement between our TST/ZCT results and the experimental ones for $500 \leq T \leq 800$ was found which supports our high temperature rate constant results for use in both atmospheric and combustion chemistry.

Acknowledgements

The authors are grateful to Prof. Donald G. Truhlar, Department of Chemistry University of Minnesota, for the license access to POLYRATE 7.3.1 program.

We Would like to thank M.A. Hajji from the Engineering School of Sfax for his help with English.

References

[1] W. Stang, R.F Hampson, J. Phys. Chem. Ref. Data 15 (1986) 1087.
[2] D.L. Baulch, C.L. Cobos, R.A. Cox, P. Frank, G. Hayman, Th. Just, J.A. Kerr, T. Murrells, M.J. Pilling, J. Troe, R.W. Walker, J. Warnatz, J. Phys. Chem. Ref. Data 24 (4) (1995) 1609.
[3] M.W. Schmidt, K.K. Baldridge, J.A. Boatz, S.T. Elbert, M.S. Gordon, J.H. Jensen, S. Koseki, N. Matsunaga, K.A. Nguyen, S.J. Su, T.L. Windus, M. Dupuis, J.A. Montgomery, J. Comput. Chem. 14 (1993) 1347.
[4] T.H. Dunning Jr., J. Chem. Phys. 90 (1989) 1007.
[5] B.O. Roos, Adv. Chem. Phys. 69 (1987) 339.
[6] H. Nakano, J. Chem. Phys. 99 (1993) 7983.
[7] H. Nakano, Chem. Phys. Lett. 207 (1993) 372.
[8] S.F. Boys, F. Bernardi, Mol. Phys. 19 (1970) 553.
[9] T.N. Truong, D.G. Truhlar, J. Chem. Phys. 93 (1990) 1761.
[10] E. Wigner, Z. Phys. Chem. B 19 (1932) 203.
[11] A. Gonzalez-Lafont, T.N. Truong, D.G. Truhlar, J. Chem. Phys. 95 (1991) 8875.
[12] R. Steckler, Y.Y. Chuang, P.L. Fast, E.L. Coitino, J.C. Corchado, W.P. Hu, Y.P. Liu, G.C. Lynch, K.A. Nguyen, C.F. Jackels, M.Z. Gu, I. Rossi, V. Clayton, S. Mellissas, B.C. Garrett, B.C. Garrett, A.D. Issacson, D.G. Truhlar, POLYRATE-version 7.3.1, University of Minnesotta, Minneapolis, 1997.
[13] R. Fourier, A.E. De Pristo, J. Chem. Phys. 96 (1992) 1183.
[14] Y. Tarchouna, M. Bahri, N. Jaïdane, Z. Ben Lakhdar, J.P. Flament, J. Chem. Phys. 118 (3) (2003) 1189.
[15] M. Bahri, N. Jaïdane, Z. Ben Lakhdar, J.P. Flament, J. Chim. Phys. 96 (1999) 634.
[16] T.N. Truong, D.G. Truhlar, J. Chem. Phys. 93 (1990) 1761.
[17] V.S. Melissas, G. Truhlar, J. Phys. Chem. 98 (1993) 875.
[18] K.D. Dobbs, D.A. Dixon, A. Komornicki, J. Chem. Phys. 98 (1993) 8852.
[19] M.W. Chase Jr, C.A. Davies, J.R. Downey Jr, D.J. Frurip, R.A. Mc Donald, A.N. Syverud (Eds.), JANAF Thermodymamical Tables, third ed., vol. 14, National Bureau of Standards, Washington, DC, 1985.
[20] M.E. Jacox, Vibrational and Electronic Energy Levels of Polyatomic Transient Molecules, AIP, Woodbury, 1994.
[21] T. Shimanouchi, Table of molecular vibrational frequencies, Consolidated Vol.1, NSRDS NBS-39.
[22] J.A. Boatz, M.S. Gordon, J. Phys. Chem. 93 (1989) 1819.
[23] B. Ruscic, A.F. Wagner, L.B. Harding, R.L. Asher, D. Feller, D.A. Dixon, K.A. Peterson, Y. Song, X. Qian, C.-Y. Ng, J. Liu, W. Chen, W. Schwenke, J. Phys. Chem. A 106 (2002) 2727.
[24] H. Richard Holgate, J.W. Tester, J. Phys. Chem. 98 (1994) 810.